Biogeochemistry (2018) 137:197–217
https://doi.org/10.1007/s10533-017-0411-0

Stable calcium isotope speciation and calcium oxalate production within beech tree (*Fagus sylvatica* L.) organs

Anne-Désirée Schmitt · Natalia Borrelli · Damien Ertlen · Sophie Gangloff · François Chabaux · Margarita Osterrieth

Received: 10 July 2017 / Accepted: 11 December 2017 / Published online: 4 January 2018

Abstract In this study, we linked Ca speciation with isotope composition in plants. To do this, we performed leachate experiments to access the soluble Ca, structurally bound Ca and insoluble Ca (i.e., water and weak acid resistant) within beech tree organs (*Fagus sylvatica* L.). Ca isotopic measurements were combined with infrared spectroscopy and calcium oxalate biomineralization identification. The results from our study indicate that bark and leaves are the most enriched in monohydrated calcium oxalate crystals (whewellite), which are observable in parenchyma and sclerenchyma tissues, whereas roots and wood are enriched in structurally bound Ca. Our leaching experiments also show decreasing $\delta^{44/40}$Ca isotopic signatures in the order of soluble Ca > structurally bound Ca > insoluble Ca. This finding implies that because leaves degrade faster than wooden organs and because Ca linked to pectate decomposes faster than Ca linked to oxalate crystals, differential Ca isotopic signatures are expected to be observed during litter degradation.

Keywords Beech tree · Ca isotopes · Ca-oxalate crystals · Ca-soluble · Ca-structurally bound · FTIR

Responsible Editor: Jonathan Sanderman.

A.-D. Schmitt (✉) · S. Gangloff · F. Chabaux
Université de Strasbourg, CNRS-UMR 7517, LHyGeS/EOST, 1, rue Blessig, 67084 Strasbourg Cedex, France
e-mail: adschmitt@unistra.fr

N. Borrelli · M. Osterrieth
Instituto de Geología de Costas y del Cuaternario, FCEyN, UNMdP-CIC, CC722 (7600), Mar del Plata, Buenos Aires, Argentina

N. Borrelli · M. Osterrieth
Instituto de Investigaciones Marinas y Costeras, CONICET-UNMdP, Mar del Plata, Buenos Aires, Argentina

D. Ertlen
Université de Strasbourg, CNRS-UMR 7362, Image, Ville, Environnement, 3, rue de l'Argonne, 67083 Strasbourg, France

Introduction

Calcium (Ca) is a ubiquitous macronutrient, the sixth most important element in plants (per gram of dry matter) and essential for plant growth. Ca forms bonds preferentially with oxygen in the cell membranes and walls, as well as with lightly loaded ligands. This characteristic may explain the ability of Ca to bind with proteins and enzymes (Roberts et al. 1992), which implies that Ca has several important functions in plant cells: it is important for the formation and stability of cell wall structures by cross-linking pectin chains, it controls the activity of wall enzymes, it acts as a counter-cation for inorganic and organic anions in the vacuole, and it acts as a universal secondary messenger in a variety of cells (Marschner 1995;

McLaughlin and Wimmer 1999; White and Broadley 2003; Amtmann and Blatt 2009; Taiz and Zeiger 2010). In addition, Ca^{2+} is one of the main components of many biomineralizations in the plant kingdom (e.g., Ca-tartrate, Ca-malate, Ca-citrate, Ca-phosphate, Ca-oxalate, Ca-carbonate), and among them, calcium oxalate crystals (COCs) are the most widespread (e.g., Bauer et al. 2011). These crystals are formed by the precipitation of Ca, which is taken up by roots from soil sources and biologically synthesized oxalate in the vacuoles of the idioblasts of all vegetative and reproductive organs mainly in epidermal and parenchyma tissues. COCs occur either as monohydrate (whewellite, $CaC_2O_4{\cdot}H_2O$) or dihydrate (weddellite, $CaC_2O_4{\cdot}2H_2O$) crystals, and the most frequent morphologies are druses (spherical multifaceted conglomerate crystals), rhombohedral or prismatic crystals (block-like crystals), styloids (large elongate rectangular crystals), raphides (bundles of needle shaped crystals) and crystal sand (masses of small angular crystals) (Franceschi and Nakata 2005). COCs play essential structural and physiological functions in plants: they prevent Ca accumulation around the chlorenchyma cells, ensuring their cellular functions; enhance the diffraction of light; protect against herbivory and chewing insects; and, in seeds, serve as a Ca store for the embryo (Ilarslan et al. 1997; Prychid and Rudall 1999; Molano-Flores 2001; Hudgins et al. 2003; Braissant et al. 2004; Franceschi and Nakata 2005; Korth et al. 2006; Horner 2012). Upon the death and decay of plants, COCs become part of the litter. The decomposition of litter is an essential process that controls both recycling and nutrient availability in forested ecosystems (Likens et al. 1998; Dijkstra 2003; Liao et al. 2006). Once plants decay, COCs are sparingly soluble in the typical pH range of soils (Cromack et al. 1979; Gadd 1999; Bailey et al. 2003). Nevertheless, COC solubility may increase with increasing ionic strength of the solution (the so-called neutral salt effect), and near-complete dissolution is also observed in strong acids (Mendham et al. 2000; Belliveau and Griffin 2001; Dauer and Perakis 2013). Moreover, oxalotrophic bacteria, which are common in trees and litter, promote the oxidation of oxalate minerals because they function as carbon, energy and electron sources, thus influencing the carbon and calcium cycles in soils (Braissant et al. 2004; Verrecchia et al. 2006).

Recent studies have discussed the Ca isotopic composition of bulk tissues (soluble, structurally bound or insoluble) (Cobert et al. 2011; Bagard et al. 2013; Schmitt et al. 2013, 2017). Cobert et al. (2011) have especially suggested lower $\delta^{44/40}$Ca isotopic compositions in COCs based on a preliminary strong acid leachate of a bean leaf. Bullen confirmed such low $\delta^{44/40}$Ca values in COCs by other experiments (pers.com.). Therefore, knowledge of the Ca isotopic compositions of various forms in which we find Ca in plants will help to identify the isotopic signatures that return to the soil during recycling. To check for possible source variations within tree organs, we combine Ca isotopes ($\delta^{44/40}$Ca) with radiogenic Sr isotopes ($^{87}Sr/^{86}Sr$,), which are recognized as tracers of Ca sources and mixture processes for some organs (Graustein 1989; Åberg et al. 1989; Miller et al. 1993; Kendall et al. 1995; Bailey et al. 1996; Capo et al. 1998; Blum et al. 2002; Kennedy et al. 2002; Bullen and Bailey 2005; Drouet et al. 2005; Bélanger et al. 2012; Bedel et al. 2016). While there are numerous studies reporting the presence of COCs in plants, few refer to the Fagaceae family (Trockenbrodt 1995; Lersten and Horner 2008; Serdar and Demiray 2012) and especially to *Fagus sylvatica* L. In particular, since the research of Lersten and Horner (2008) and Krieger et al. (2017) in which the macropattern COCs of organs of this beech family were reported, this is the first report on the relationships of COCs with Ca biogeochemistry through the combined study of COC macropatterns, infrared spectroscopy and isotope compositions in vegetative and reproductive organs of *Fagus sylvatica* L. We focus on the beech tree (*Fagus sylvatica* L.) organs from the Strengbach catchment, the bulk isotopic compositions of which have been previously analysed (Schmitt et al. 2017). The objectives of this study are threefold:

(1) Determine the isotopic compositions of the different Ca forms (soluble Ca, structurally bound Ca, insoluble Ca) encountered in different beech tree organs;
(2) Identify and spectroscopically characterize Ca-oxalate biomineralizations encountered in different beech tree organs; and
(3) Relate the isotopic fractionation of calcium in plants to the production of calcium oxalate biomineralizations and soil biogeochemistry.

Materials and methods

Site description

The Strengbach forested catchment (80 ha) is in the Vosges mountains (NE France), approximately 60 km south of Strasbourg (48°12′N; 7°11′E). This catchment is characterized by elevations between 880 m and 1150 m a.s.l. and steep slopes (15° on average) (Fig. 1). The climate is temperate oceanic-mountainous, with a mean annual temperature of 6 °C, temperatures ranging from − 2 °C in January to 14 °C in August (Probst et al. 1990), a mean annual precipitation of 1400 mm and a mean annual runoff of 814 mm (Viville et al. 2012). The bedrock of the catchment is a Ca-poor (less than 1%), Hercynian leucogranite (the Brézouard granite, aged 322 ± 2 Ma; Boutin et al. 1995) with a small area of gneiss at its northern edge. The soils are rather deep (80–100 cm on average), sandy and stony and vary from Dystric Cambisol to Albic Podzol (Fichter et al. 1998a, b; WRB 2014). The forest covers 85% of the catchment area and is a mixture of 80% Norway spruce (*Picea abies* L.) and 20% European beech (*Fagus sylvatica* L.). The remaining area corresponds to clearings and a wetland near the catchment's outlet. Two experimental sites cover the catchment and are described as follows: the northern slope spruce plot (VP) is covered with 115-year-old spruce trees, and the southern slope beech plot (HP) is covered with 175-year-old beech trees.

Sample description

Leachate samples from several beech tree organs (see Table 1) collected in September 2011 and June 2012 from the HP plot in the Strengbach catchment were studied in this paper. Bulk stable Ca and radiogenic Sr isotopes of the same samples have been previously analysed (Schmitt et al. 2017). All beech tree organs were carefully washed with ultrapure Millipore® water in the LHyGeS laboratory. The roots were ultra-sonicated in several ultrapure water baths to remove the attached soil micro fragments. The quality of the cleaning was assessed by verification with a binocular microscope. The first outer millimetre of the bark was removed to prevent atmospheric contamination and lichen coatings (Catinon et al. 2008). An aliquot of each of the different organs was saved; another part was dried at 60 °C in an oven and then reduced to powder with a specific clean agate disk mill.

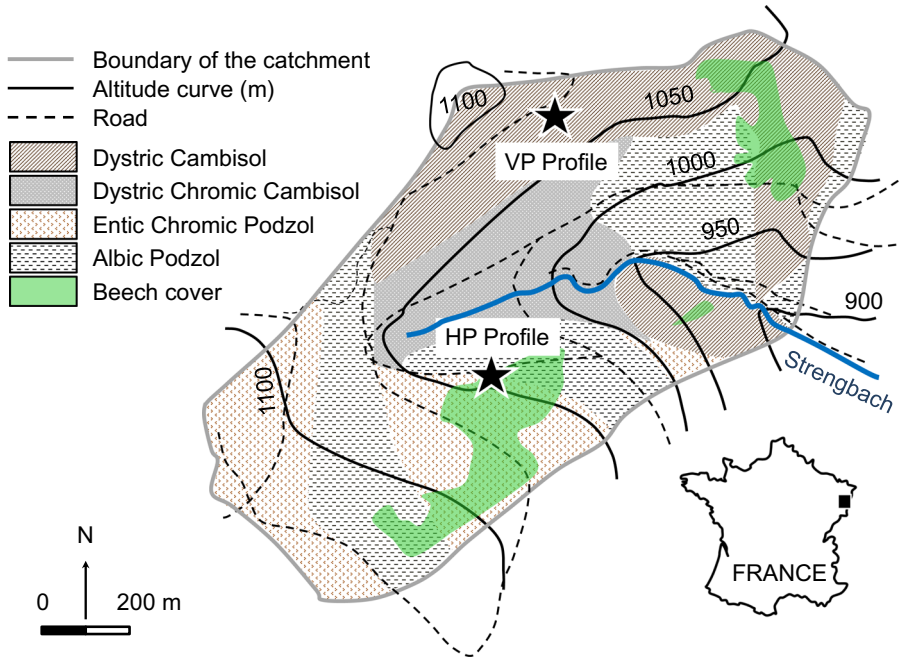

Fig. 1 Pedologic map of the Strengbach catchment. The beech cover and the location of the experimental plot under beech trees (HP) and spruce trees (VP) are also presented (modified after El Gh'Mari 1995)

Table 1 Description of samples and performed tasks

Organ	Ref.	Description	Leaching	Infra-red characterisation	Oxalate characterisation
Root	R-Q1	Close to the strain, suberized, large (2011)	x	x	x
	R-P1	Far from the strain, suberized, large (2011)	x	x	
	R-O1	Close to the strain, suberized, medium (2011)	x	x	
	R-LO	Close to the strain, suberized, small (2011)	x	x	
	R-sub	Average suberized, small (2012)	x	x	x
	R-myc	Average mycorrhized, small (2012)	x	x	x
	R-L1	Close to the strain, mycorrhized, small (2011)			x
Wood	W-TL1	Average section (sapwood + duramen) (2011)	x	x	x
Bark	B-Bk1	Cleaned of external part of suber (2011)	x	x	x
Branch	Br-1.4	Bottom, far from the trunk (2011)			x
Twigs	T-AA	Bottom, close to the trunk (2011)			x
	T-E	Top, close to the trunk (2011)			x
Leaves	L-fapic	Top, average (2012)	x	x	x
	L-D	Top, close to the trunk (2011)	x	x	
	L-G	Bottom, average (2011)	x	x	
	L-J	Bottom, far from the trunk (2011)	x	x	x
	L-f3.4p	Bottom, close to the trunk (2012)	x	x	x
	L-f3.4l	Bottom, far from the trunk (2012)			x
Seed	S-HH	Top, average (2011)	x	x	x

Leachate experiments

Powdered beech tree organs (Table 1) were subjected to a sequential extraction technique to separate Ca into soluble Ca^{2+} ions, structurally bound Ca, and insoluble Ca (i.e., water and weak acid resistant) in the LHyGeS laboratory following previously published protocols (Fink 1991; Borer et al. 2004; Dauer and Perakis 2014). The leaching procedure was processed at room temperature in polypropylene centrifuge tubes, and the samples were continuously shaken during the leachate protocol. Approximately 4 g of powder was first extracted with 30 mL of Milli-Q water, then with 30 mL 2 N acetic acid, and finally with 30 mL 2 N HCl. Hereafter, we refer to the different leachate steps as L1, L2 and L3, respectively. The L2 and L3 leachate steps were followed by two 10 mL H_2O rinses that were recovered and added to the previous acid leachate to avoid contamination from one leachate to the next. Each collected fraction was centrifuged, and the supernatant was filtered through a 0.22 µm cellulose acetate filter.

Infrared spectra

Infrared spectra were obtained at the UMR Image, Ville, Environnement laboratory in Strasbourg to identify the presence of COCs in selected beech organs (Table 1). Dried, ground beech organs were placed in a macro-cup (diameter of 5 mm) and scanned from 4000 to 450 cm^{-1} with an IR Frontier Spectrometer with a KBr beam splitter, a diffuse reflectance sampling accessory and a TGS detector (PerkinElmer, USA). The measured reflectance (R) was transformed into absorbance (A) using the following relationship:

$$A = \log(1/R) \quad (1)$$

Calcium oxalate crystals

Description and quantification of COCs in the beech tree organs (Table 1) were performed at the Instituto de Geología de Costas y del Cuaternario in Buenos Aires. Cross sections of roots, branches, seeds and bark were cleared with 50% (w/v) sodium

hypochlorite. Leaves were diaphanized (Dizeo de Strittmater 1973), and because of their area and thickness, it was possible to calculate the crystal density (number of crystals per mm^2 of leaf area) by counting all the crystals within an area of 0.115 mm^2. Approximately 14 regions in three leaves of each sample were counted, with a total area counted of 1.61 mm^2 per leaf. All the material was mounted with gelatine–glycerine, and the COCs were identified and described with an optical microscope (Leitz Wetzler D35780) at 100× to 400× magnification. To analyse the size of the crystals, approximately 30–80 crystals per sample were measured, depending on the COC production of the different organs studied. Differences in the length and density of the prismatic crystals among the different types of leaves were tested by a Kruskal–Wallis test and a non-parametric multiple comparison test because normality and homoscedasticity assumptions were not achieved (Zar 1984).

Elemental and isotopic measurements

Elemental and isotopic measurements were performed following standard procedures commonly used in the LHyGeS at Strasbourg (Lahd Geagea et al. 2008; Schmitt et al. 2009; Prunier et al. 2015; Gangloff et al. 2016; Schmitt et al. 2017). Ca and Sr concentrations were measured, respectively, by ICP-AES (Thermo Scientific iCAP 6000 SERIES—Thermo Fisher Scientific©, Waltham, MA) and ICP-MS (Thermo Fisher Scientific©, Waltham, MA) with traditional calibration, indium as the internal standard and uncertainty between ± 5 and 10%. The blank for each element was equal to 1–5% of the concentration of the sample. The accuracy of the measurement was verified by certified standard measurements (SLRS5, Perade-20, Rain 97, and Big-Moose 02).

Elution of Sr with Sr spec resin was performed using 0.05 N HNO_3 (e.g., Lahd Geagea et al. 2007), and the isotopic ratios were determined by thermo-ionization on a Thermo Scientific (Thermo Electron Scientific©, Waltham, MA) Triton mass spectrometer (TIMS) with an average analytical uncertainty of ± 0.00001 (2SE). The $^{87}Sr/^{86}Sr$ value of the routinely measured NIST NBS 987 standard was equal to 0.710242 ± 0.000007 during the study (2SD, N = 9).

Ca isotopic compositions were determined following the procedure described by Schmitt et al. (2009, 2013). The Ca isotope values are expressed as a per-mil deviation relative to the NIST SRM 915a standard solution (Eisenhauer et al. 2004):

$$\delta^{44/40}\mathrm{Ca}\ (‰) = \left\{ \left({}^{44}\mathrm{Ca}/{}^{40}\mathrm{Ca} \right)_{\mathrm{sample}} \Big/ \left({}^{44}\mathrm{Ca}/{}^{40}\mathrm{Ca} \right)_{\mathrm{SRM915a}} - 1 \right\} \times 1000 \quad (2)$$

The external reproducibility of the $\delta^{44/40}Ca$ values is 0.11‰ (2SD) based on repeated measurements of the NIST SRM 915a (N = 42) and 0.12‰ (2SD) based on the replicate sample measurements (N = 36), including several sample matrixes. Our measurements thus have an uncertainty of ± 0.11‰. To improve the statistical significance of a single $\delta^{44/40}Ca$ measurement, the Ca isotope data are generally a combination of two individual measurements, including Ca purification by ion chromatography and TIMS analyses. The accuracy of the measurements was tested by measurements of seawater during the same period (1.84 ± 0.10‰, 2SD; N = 19), and the values were in good agreement with the previously published values (Hippler et al. 2003). Total Ca blanks for the isotope analyses were less than 3%, and blank corrections were not necessary.

Results

Leachate experiments

Elemental and isotopic compositions of calcium and strontium in the different leachates are reported in Table 2 and Fig. 2. The reference names of the different organs are presented in Table 1. The Ca concentrations are higher in bark, leaves and seeds than in root and wood organs in L3 and in L2 and L1 leachates (Fig. 2a). Maximal calcium concentrations are recorded in the L3 leachate for bark and basal leaves collected close to the trunk in 2012 (L-f3.4p). Considering the L2 leachate, peak Ca concentrations are observed for a small mycorrhized sample from 2012 (R-LO), followed by bark and seed samples, leaf samples and then the other organ samples. For the L1 leachate, Ca concentrations in the leaves (17.5 ± 2.3 mmol/g, on average, 2SE, N = 5) are higher than in other organs (4.2 ± 1.2 mmol/g, on average, 2SE, N = 9). Overall, Ca concentrations of the L2 leachates are higher than those of L1 leachates. Particularly, Ca in roots, seeds and wood organs is

Table 2 Calcium and strontium elemental and isotopic compositions of the different leachates

Organ	Lab. numb.	Ref.	Description	Ca (mmol/g)	SD[a] (mmol/g)	$\delta^{44/40}Ca_1$ (‰)	$\delta^{44/40}Ca_2$ (‰)	$\delta^{44/40}Ca_{average}$ (‰)	2SD[b] (‰)	$^{87}Sr/^{86}Sr$	2SE[c]
L1											
Root	13-1*	R-Q1	Close to the strain, suberized, large (2011)	2.25	0.47	0.54	–	0.54	0.12	0.72944	0.00001
										0.72948	0.00001
	15-1	R-P1	Far from the strain, suberized, large (2011)	2.22	0.47	0.39	–	0.39	0.12	0.72779	0.00001
										0.72777	0.00001
										0.72780	0.00001
	6-1	R-O1	Close to the strain, suberized, medium (2011)	4.61	0.68	0.40	–	0.40	0.12	–	–
	17-1	R-LO	Close to the strain, suberized, small (2011)	6.00	0.77	0.41	0.40	0.41	0.08	0.72034	0.00001
	14-1	R-sub	Average suberized, small (2012)	6.93	0.83	0.34	–	0.34	0.12	–	–
	16-1	R-myc	Average mycorrhized, small (2012)	3.34	0.58	0.36	0.38	0.37	0.08	–	–
Wood	5-1	W-TL1	Average section (sapwood + duramen) (2011)	2.78	0.53	0.03	–	0.03	0.12	–	–
Bark	3-1*	B-Bk1	Cleaned of external part of suber (2011)	2.96	0.54	− 0.04	–	− 0.04	0.12	–	–
Leaves	4-1	L-fapic	Top, average (2012)	17.2	1.3	1.11	–	1.11	0.12	–	–
	7-1	L-D	Top, close to the trunk (2011)	13.3	1.2	0.63	–	0.63	0.12	–	–
	8-1	L-G	Bottom, average (2011)	19.4	1.4	0.58	–	0.58	0.12	–	–
	2-1*	L-J	Bottom, far from the trunk (2011)	19.4	1.4	0.79	–	0.79	0.12	0.72713	0.00001
	1-1*	L-f3.4p	Bottom, close to the trunk (2012)	18.4	1.4	0.82	–	0.82	0.12	–	–
Seed	9-1	S-HH	Top, average (2011)	6.41	0.80	0.86	–	0.14	0.14	–	–
L2											
Root	13-2*	R-Q1	Close to the strain, suberized, large (2011)	12.1	1.6	0.39	0.14	0.27	0.08	0.73089	0.00001
	15-2	R-P1	Far from the strain, suberized, large (2011)	14.0	1.8	0.18	0.03	0.11	0.08	0.72923	0.00001
	6-2	R-O1	Close to the strain, suberized, medium (2011)	33.6	3.8	− 0.17	− 0.05	− 0.11	0.08	–	–
	17-2	R-LO	Close to the strain, suberized, small (2011)	46.9	5.2	0.02	–	0.02	0.12	0.72035	0.00001

Table 2 continued

Organ	Lab. numb.	Ref.	Description	Ca (mmol/g)	SD[a] (mmol/g)	$\delta^{44/40}Ca_1$ (‰)	$\delta^{44/40}Ca_2$ (‰)	$\delta^{44/40}Ca_{average}$ (‰)	2SD[b] (‰)	$^{87}Sr/^{86}Sr$	2SE[c]
	14-2	R-sub	Average suberized, small (2012)	13.6	1.8	− 0.09	− 0.25	− 0.17	0.08	–	–
	16-2	R-myc	Average mycorrhized, small (2012)	5.33	0.90	0.10	0.11	0.11	0.08	–	–
Wood	5-2	W-TL1	Average section (sapwood + duramen) (2011)	21.0	2.5	− 0.15	0.04	− 0.06	0.08	–	–
Bark	3-2*	B-Bk1	Cleaned of external part of suber (2011)	72.6	7.7	− 0.24	− 0.07	− 0.16	0.08	–	–
Leaves	4-2	L-fapic	Top, average (2012)	24.3	2.9	0.57	–	0.57	0.12	–	–
	7-2	L-D	Top, close to the trunk (2011)	38.6	4.3	0.59	–	0.59	0.12	–	–
	8-2	L-G	Bottom, average (2011)	38.0	4.3	0.57	–	0.57	0.12	–	–
	2-2*	L-J	Bottom, far from the trunk (2011)	40.2	4.5	0.50	0.54	0.52	0.08	0.72717	0.00001
	1-2*	L-f3.4p	Bottom, close to the trunk (2012)	36.8	4.2	0.46	0.63	0.55	0.08	–	–
Seed	9-2	S-HH	Top, average (2011)	63.4	6.8	0.37	–	0.37	0.12	–	–
L3											
Root	13-3*	R-Q1	Close to the strain, suberized, large (2011)	1.90	0.48	0.13	–	0.13	0.12	0.73095	0.00007
	15-3	R-P1	Far from the strain, suberized, large (2011)	3.08	0.63	− 0.23	–	− 0.23	0.12	0.72918	0.00001
										0.72918	0.00001
	6-3	R-O1	Close to the strain, suberized, medium (2011)	32.0	3.7	− 0.67	–	− 0.67	0.12	–	–
	17-3	R-LO	Close to the strain, suberized, small (2011)	5.13	0.88	− 0.68	–	− 0.68	0.12	0.72182	0.00001
										0.72183	0.00001
	14-3	R-sub	Average suberized, small (2012)	4.36	0.79	− 0.32	–	− 0.32	0.12	–	–
	16-3	R-myc	Average mycorrhized, small (2012)	2.55	0.57	− 0.08	− 0.11	− 0.10	0.08	–	–
Wood	5-3	W-TL1	Average section (sapwood + duramen) (2011)	4.74	0.84	− 0.22	− 0.31	− 0.27	0.08	–	–
Bark	3-3*	B-Bk1	Cleaned of external part of suber (2011)	293	30	− 0.82	− 0.87	− 0.85	0.08	–	–
Leaves	4-3	L-fapic	Top, average (2012)	58.4	6.3	− 0.10	− 0.12	− 0.11	0.08	–	–
	7-3	L-D	Top, close to the trunk (2011)	50.1	5.5	0.24	–	0.24	0.12	–	–
	8-3	L-G	Bottom, average (2011)	98.3	10.3	− 0.03	–	− 0.03	0.12	–	–
	2-3*	L-J	Bottom, far from the trunk (2011)	107	11	0.07	0.15	0.11	0.08	0.72709	0.00008

Table 2 continued

Organ	Lab. numb.	Ref.	Description	Ca (mmol/g)	SD[a] (mmol/g)	$\delta^{44/40}Ca_1$ (‰)	$\delta^{44/40}Ca_2$ (‰)	$\delta^{44/40}Ca_{average}$ (‰)	2SD[b] (‰)	$^{87}Sr/^{86}Sr$	2SE[c]
	1-3*	L-f3.4p	Bottom, close to the trunk (2012)	205	27	0.00	–	0.00	0.12	–	–
Seed	9-3	S-HH	Top, average (2011)	55.8	6.1	− 0.18	− 0.22	− 0.20	0.08	–	–

* Calculated from replicate leachates

[a]Calculated using error propagation

[b]External long-term 2SD based on replicate measurements

[c]Internal 2SE reproducibility

mainly structural (L2), whereas in bark and leaves, calcium mainly occurs in an insoluble form (L3) (Table 2).

For Ca isotopes (Fig. 2b and Table 1), L1 leachates have greater $\delta^{44/40}$Ca values than L2 and L3 leachates, the latter having the lowest $\delta^{44/40}$Ca values. For L1 and L2 leachates, leaves have higher $\delta^{44/40}$Ca values (0.79 ± 0.19‰; 2SE; N = 5 and 0.56 ± 0.02‰; 2SE; N = 5, respectively) compared to the other organs (0.41 ± 0.06‰; 2SE; N = 6 and 0.02 ± 0.10; 2SE; N = 9, respectively). Finally, for the L3 leachate, the organs present relatively homogenous Ca isotopic compositions (-0.08 ± 0.11‰; 2SE; N = 11), except for medium and small roots and bark (-0.73 ± 0.11‰; 2SE; N = 3).

Considering the Sr isotopes are based on a small dataset, we observe that for large roots, L2 and L3 Sr isotopic compositions are similar and more radiogenic than those of L1 leachates (Fig. 2c). In contrast, for small roots, L1 and L2 Sr isotopic signatures are similar and less radiogenic than those of L3 leachates. Finally, for leaves, no Sr isotopic variation was recorded within the different leachates.

Infrared spectra

Infrared spectroscopy is a powerful tool for investigating plant biominerals (Monje and Baran 1996, 1997, 2005; Baran and Rolleri 2009; Schmitt et al. 2012). In the present study, we implemented this technique for the first time to identify Ca-forming crystals, especially Ca-oxalate crystals, in beech tree organs. The infrared spectra of different beech tree organs appear quite similar (Fig. 3a), except for those of the seed sample (S-HH). This difference is mainly due to the physical properties of the S-HH sample, which could not be powdered properly because of its elevated oil content; this sample will not be discussed hereafter. The other samples show a broad peak between 3550 and 3250 cm^{-1}, a smaller peak at 2900 cm^{-1}, a group of peaks in the 1000–1800 cm^{-1} region and a group of small peaks at approximately 600 cm^{-1} (Fig. 3a). The spectra are obtained from bulk beech organs, which are chemically heterogeneous. The broad peaks centred at approximately 3400 cm^{-1} are certainly related to the H–O–H stretches of the crystal water in the calcium oxalate and/or to the Si–OH groups (Christy et al. 1994; Baran and Rolleri 2010). In our study, because the 600 cm^{-1}

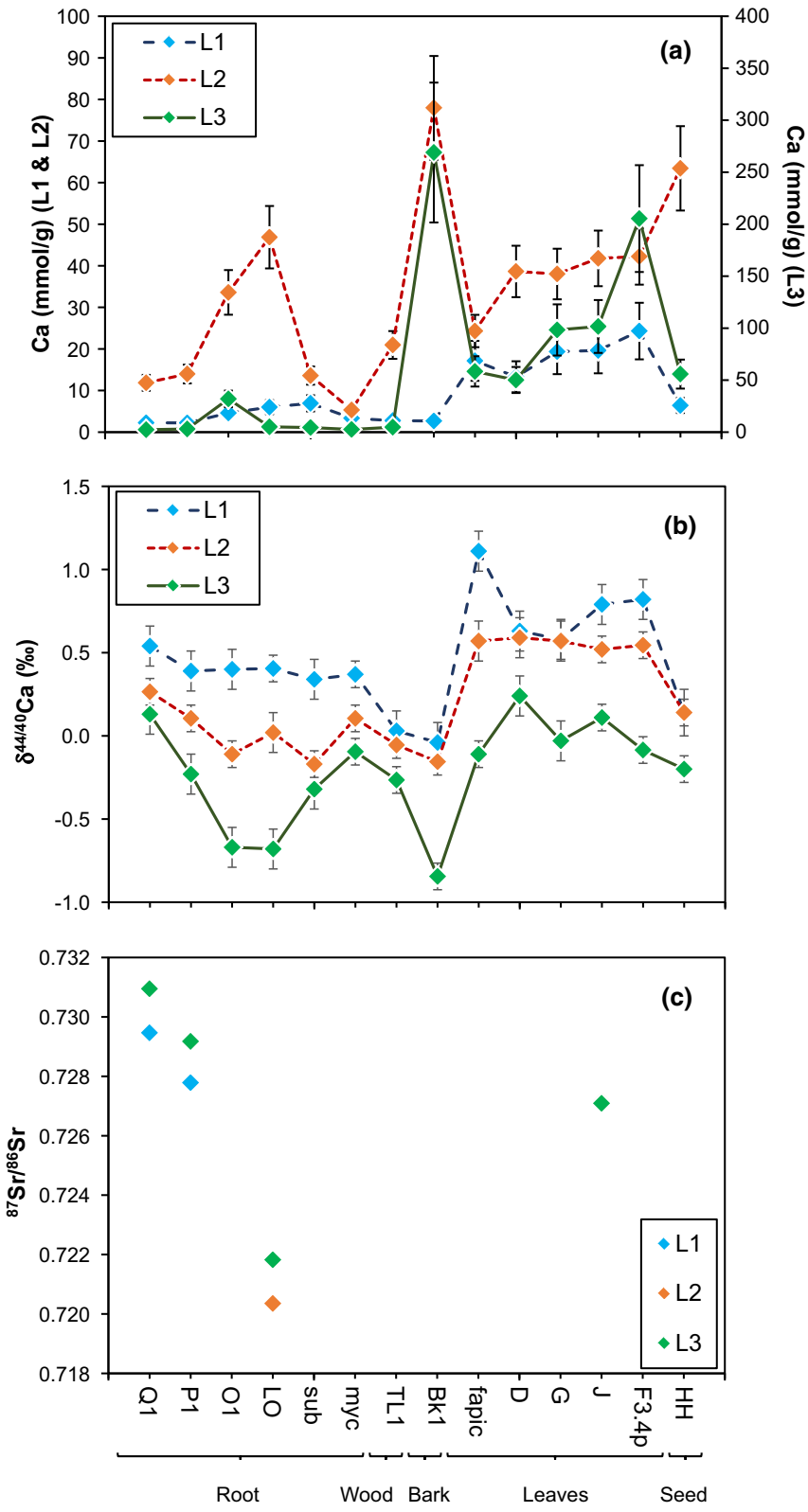

Fig. 2 Variations in **a** calcium concentrations, **b** $\delta^{44/40}$Ca (‰), and **c** $^{87}Sr/^{86}Sr$ in the studied organs. The uncertainties represent the error bars given in Table 3. *L* leaf, *R* root, *B* bark, *S* seed

Table 3 Proportion of Ca in each leachate and determination of $\delta^{44/40}Ca_{total}$ (‰)

Organ	Lab. numb.	Ref.	Ca-L1[a] (%)	SD-1[b] (%)	Ca-L2[a] (%)	SD-2[b] (%)	Ca-L3[a] (%)	SD-3[b] (%)	$\delta^{44/40}Ca^{c}_{total}$ (‰)	SD-total[b] (‰)	$\delta^{44/40}Ca^{d}_{bulk}$ (‰)	2SD[d] (‰)
Root	13	R-Q1	13.8	11.1	72.3	53.4	13.9	11.5	0.29	0.49	0.30	0.08
	15	R-P1	11.5	4.5	72.5	25.3	16.0	6.1	0.09	0.10	0.12	0.08
	6	R-O1	6.6	1.7	47.9	11.8	45.6	11.2	− 0.33	0.30	− 0.27	0.08
	17	R-LO	10.3	2.8	80.8	21.4	8.8	2.6	0.00	0.01	− 0.07	0.08
	14	R-sub	27.8	7.8	54.6	15.7	17.5	5.5	− 0.05	0.05	− 0.08	0.08
	16	R-myc	29.7	11.0	47.5	17.6	22.8	9.0	0.14	0.18	0.00	0.08
Wood	5	W-TL1	9.8	3.3	73.6	22.9	16.6	5.6	− 0.09	0.37	0.02	0.12
Bark	3	B-Bk1	0.8	0.5	22.5	12.0	76.8	40.5	− 0.69	2.20	− 0.62	0.12
Leaves	4	L-fapic	17.2	3.3	24.4	5.2	58.5	12.2	0.27	0.22	0.37	0.08
	7	L-D	13.0	2.6	37.9	8.0	49.1	10.3	0.42	0.29	0.34	0.08
	8	L-G	12.4	2.3	24.4	5.0	63.1	12.6	0.19	0.77	0.21	0.08
	2	L-J	12.0	4.4	25.7	10.4	62.3	24.7	0.30	0.30	0.32	0.08
	1	L-f3.4p	9.6	3.4	16.4	6.5	74.0	28.8	0.15	0.11	0.30	0.08
Seed	9	S-HH	5.1	1.2	50.5	11.4	44.4	10.0	0.11	0.12	0.13	0.08

[a]Calculated from Table 2 by assuming the sum of the leachings corresponds to the total amount of Ca

[b]Calculated using error propagation

[c]Calculated by weighting $d^{44/40}Ca$ from the three leachings with the percentage of Ca leached in each extraction

[d]From Schmitt et al. (2017)

region produces unclear and overlapping peaks, we focused our attention on the 1000–1800 cm^{-1} region, where several features typical of Ca-oxalate can be recognized, among others (Fig. 3b).

We can observe peaks between 1080 and 1170 and at 1250 and 1450 cm^{-1} for all organs, with the lowest intensity for leaves and the highest for wood (at 1250 cm^{-1}) or bark and large roots (for the other bands) (Fig. 3b, c). The 1080–1170 cm^{-1} band could represent the presence of opal SiO_2 (Perry 1989; Kamatani 1991; Baran and Rolleri 2010; Baran et al. 2010). The 1250 cm^{-1} peaks are consistent with previous results obtained for beans (Schmitt et al. 2013) but are not specifically associated with biominerals (Monje and Baran 2004). The 1450 cm^{-1} vibrational band could represent an asymmetric stretching vibration of calcium magnesium bicarbonate (Contreras-Padilla et al. 2015). The vibrational band observed at 1420 cm^{-1} (Fig. 3c) for wooden organs (W-TL1, R-P1, R-Q1; R-O1 and B-Bk1) is characteristic of the carbonate antisymmetric stretching mode of calcite ($CaCO_3$) (Monje and Baran 2004; Baran et al. 2010; Contreras-Padilla et al. 2015).

Concerning COCs, the two strongest IR bands, at approximately 1620–1660 and 1310–1330 cm^{-1} and corresponding to the antisymmetric and the symmetric carboxylate stretches, respectively, are found to agree with those of previous studies, although the spectra were measured from raw samples that were chemically heterogeneous (Christy et al. 1994; Monje and Baran 1996, 1997; Maurice-Estepa et al. 2000; Contreras-Padilla et al. 2015). Organic compounds, including biominerals such as silica phytoliths and Ca oxalates, produce peaks that extend into the mid-infrared region (Bozarth 1990; Christy et al. 1994; Baran and Rolleri 2010; Grinand et al. 2012; Schmitt et al. 2013). Thus, the spectra are composite spectra and do not depict pure oxalate crystals. The absence of sharpness in most of these peaks could be due to the overlap of one of the typical SiO_2 bands (Baran and Rolleri 2010). In the 1620–1660 cm^{-1} region, which is recognized as an antisymmetric carbonyl stretching band specific to the oxalate family (Christy et al. 1994; Maurice-Estepa et al. 2000), two tendencies are observed: (1) leaves show high peaks at 1660 cm^{-1}, with a shoulder at 1620 cm^{-1}; and (2) conversely,

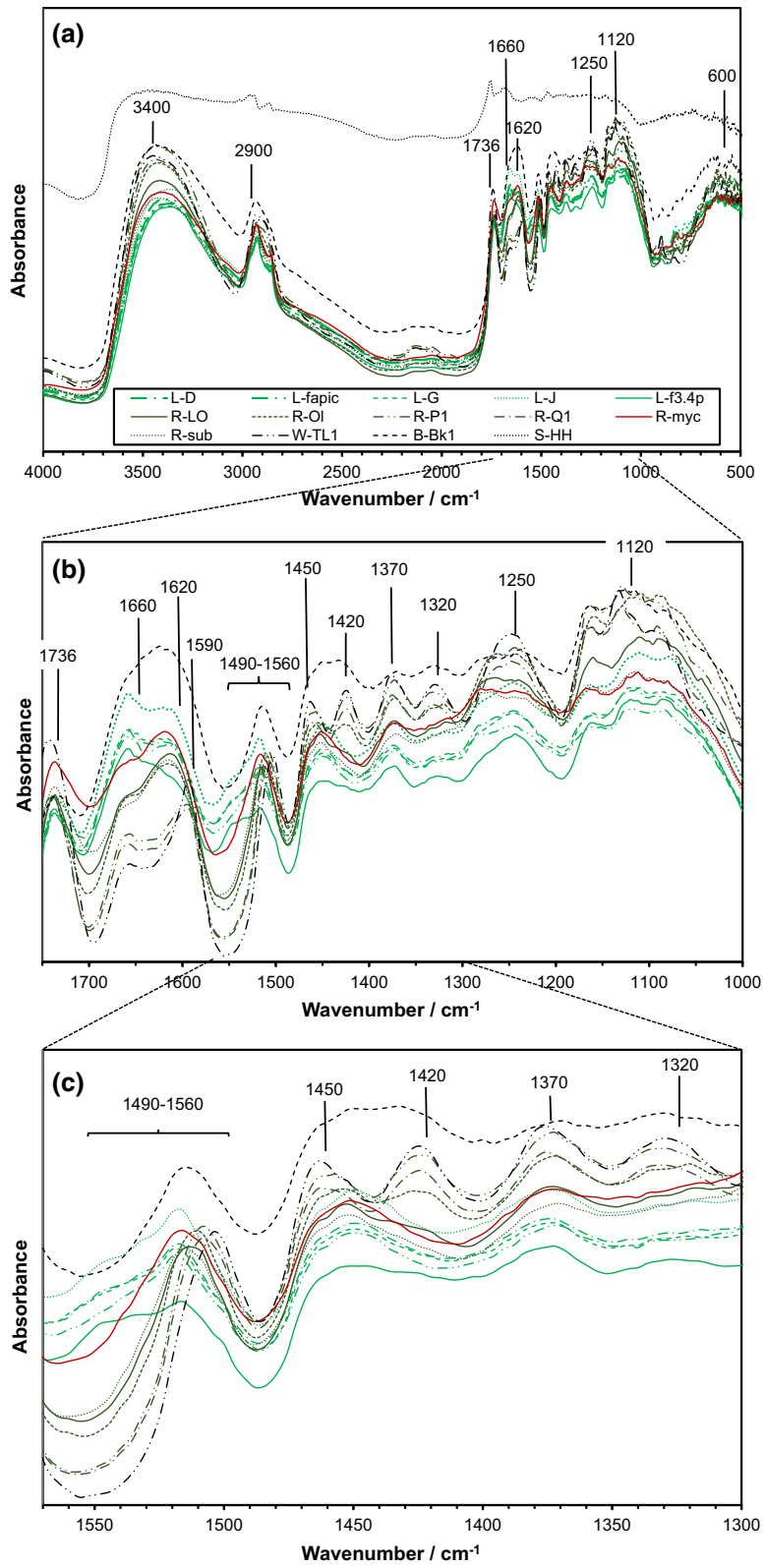

Fig. 3 Infrared spectra of beech tree organs **a** in the 500–4000 cm^{-1} region and **b** inset of the 1000-1750 cm^{-1} region, and **c** inset of the 1300–1570 cm^{-1} region

roots and wood (W-TL1) show high peaks at approximately 1620 cm^{-1}, with a shoulder at 1660 cm^{-1} (Fig. 3b). Note also that large roots (L-Q1, L-P1) and wood (W-TL1) nearly superimpose each other, with a peak slightly shifted to 1590 cm^{-1}. Bark (B-Bk1) shows only one broad peak centred at approximately 1630 cm^{-1}. The secondary carbonyl stretching band is at 1310–1330 cm^{-1}. Peaks can be observed at 1320 cm^{-1} for wood (W-TL1) and large roots (R-P1 and R-Q1). No clear peaks are identified for the other organs, with leaves having the smallest intensity of all the samples (Fig. 3c). From these two spectral regions, we can confirm the occurrence of calcium oxalate monohydrate in leaves and bark and to a lesser extent in other organs. The occurrence of calcium oxalate dihydrate is less clear because the peak for oxalate is expected at approximately 1646 cm^{-1} and because we cannot assign the peak occurring at 1660 cm^{-1} to oxalate.

Calcium oxalate crystals

Prisms and druses with central cores are the COC morphologies that are observed in all the analysed organs (Table 1). COCs are mainly located in parenchyma tissue. In roots, branches and bark (Fig. 4a, b), both prisms and druses are randomly distributed in the parenchyma of the cortex. In bark, prisms are also associated with parenchyma rays and sclerenchyma tissue (Fig. 4a, c, d), whereas in branches, druses are also associated with the medullar parenchyma and phloem. In leaves, prisms are distributed along the main vascular bundles (Fig. 4e), and druses are randomly dispersed in the mesophyll (Fig. 4f). In the seed coat, both prisms and druses are located at the parenchyma tissue between the external and internal epidermis, and prisms are associated with sclerenchyma bundles in the coat vertices.

Generally, prism lengths are within the range 8–12 μm, except in suberized roots and in the sclerenchyma of the bark, where prisms reach 25 μm in length. The diameter of druses is within a 9–20 μm range.

Bark and leaves are the organs with the highest production of COCs. Particularly in leaves, the average prism density is 307 ± 142 crystals/mm^2, but there are significant differences depending on the location of the leaf in the tree ($H = 15.25$, $p = 0.0016$, Kruskal–Wallis test). Although top leaves (L-fapic) have the highest crystal density (362 ± 169 crystals/mm^2), there are no differences with bottom leaves far from the trunk (f3.4l, 306 ± 134 crystals/mm^2, $p > 0.05$). Instead, top leaves differ from the bottom leaves close to the trunk (f3.4p, 277 ± 133 crystals/mm^2, $p = 0.01$).

Discussion

$\delta^{44/40}Ca$ signature of different Ca compounds within beech tree organs

Our leachate experiments show that the $\delta^{44/40}Ca_{total}$, calculated by weighting the Ca isotopic composition measured in each of the three extraction steps by the corresponding percentage of calcium (Table 3), is similar to the bulk Ca isotopic composition determined previously (Schmitt et al. 2017) ($R^2 = 0.92$; p value < 0.0001). This finding implies that almost all the Ca present in the different organs was extracted during this step.

The first leachate step (L1), which is characterized by the greatest $\delta^{44/40}Ca$ values, presents the most ^{44}Ca-enriched Ca isotopic signature and is supposed to provide access to water-soluble Ca (Fink 1991; Borer et al. 2004; Dauer and Perakis 2014) (Figs. 5, 6). After its entry into the apoplast, more than 90% of the Ca is adsorbed into the cell walls, whereby all the organs showed the lowest Ca proportion associated with the soluble fraction (Table 3). Free calcium transport occurs by mass flow (Clarkson 1984). Therefore, higher concentrations are supposed to be observed in organs with higher transpiration rates, i.e., leaves, where the Ca concentration in vacuoles reaches 150 mmol/L (Gilliham et al. 2011). This situation could explain the higher soluble calcium content in leaves with respect to the other organs in *Fagus sylvatica.*

The second leachate step (L2) with 2 N acetic acid, which has intermediate $\delta^{44/40}Ca$ values, is supposed to give access to the structurally bound Ca (Fink 1991; Borer et al. 2004; Dauer and Perakis 2014) (Figs. 5, 6). Within plants, Ca originating from the apoplastic circulation is present as Ca^{2+} ions associated with carboxyl (R-COOH) groups of polygalacturonic acid molecules (pectins), which are present at the exterior surface of the cell wall (in the middle lamella) by cation-exchange reactions (Bangerth 1979; Marschner

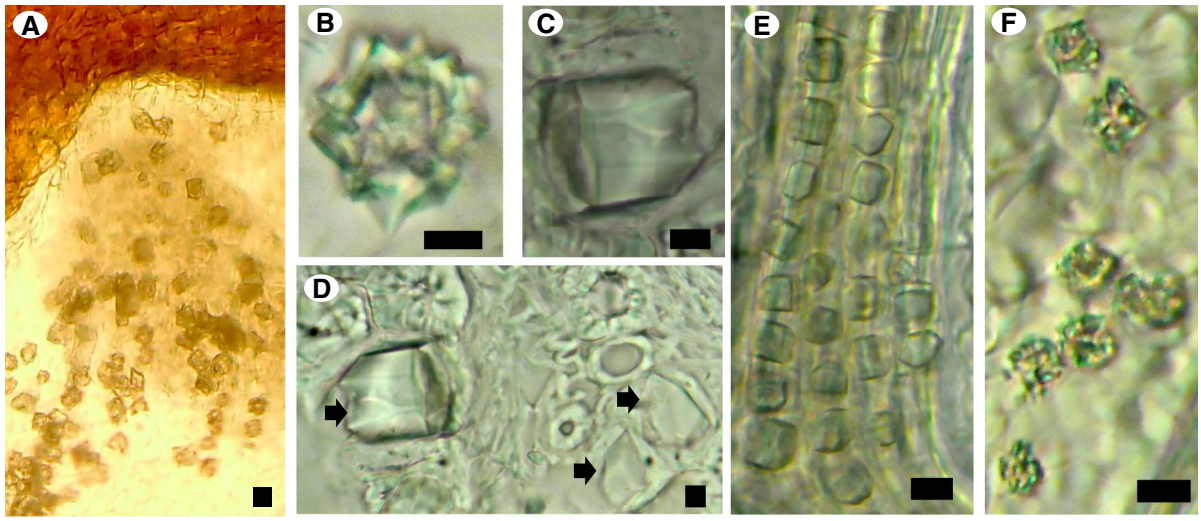

Fig. 4 Calcium oxalate crystals in bark (**a**–**d**) and leaves (**e**–**f**) of *Fagus sylvatica*. **a** General view of prisms and druses in parenchyma of the cortex. **b** Detail of a druse. **c** Detail of a prism. **d** Prisms associated with sclerenchyma (arrows). **e** Prisms associated with vascular bundles. **f** Druses in the mesophyll. Scale bar: 10 µm

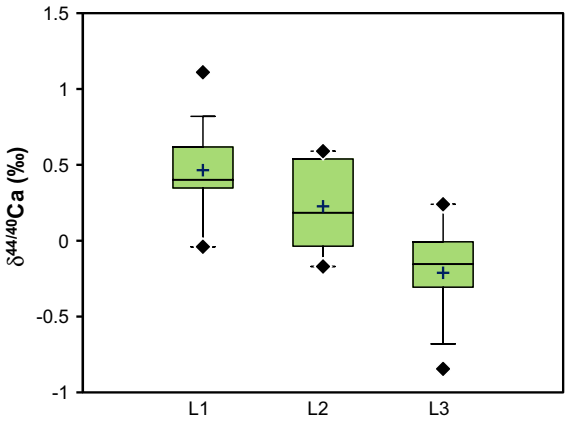

Fig. 5 Boxplot of $\delta^{44/40}$Ca corresponding to L1, L2, and L3 leachate experiments

1995; Pilbeam and Morley 2007). In doing so, Ca forms Ca bridges between two carboxyl groups of two pectin molecules, thereby contributing to the stability of the cell walls (Epstein and Bloom 2005). During this step, light ^{40}Ca is fixed on the carboxyl group in the following reaction (Cobert et al. 2011; Schmitt et al. 2013; Bagard et al. 2013; Schmitt et al. 2017):

$$2R - COOH + {}^{40}Ca^{2+} \rightarrow R - COO - {}^{40}Ca - OOC - R + 2H^{+} \quad (3)$$

Therefore, calcium has a structural role not only in the walls but also in the cell membranes by binding to the phosphate groups and to the hydroxyl (R-OH) and carboxyl groups of phenolic or uronic acids in the lignin-carbohydrate complexes and the proteins (Ito and Fujiwara 1968; Caldwell and Haug 1981; Inanaga and Okasaka 1995). Because approximately one-third of the macromolecules in the primary cell wall are pectins (Willats et al. 2001), this finding suggests that a large proportion occurs as calcium pectate. This important function of Ca in stabilizing the membranes and cell walls is relevant in roots and wood, both of which are organs with the highest portion of Ca in their structural fraction (Table 3). The results of our leachate experiments with acetic acid indicate that some of the organs enriched in Ca during the second extraction step (roots and wood) are also those where calcium carbonate was recognized by FTIR. Because weak acetic acid easily dissolves calcium carbonate, one could suggest that the higher Ca concentrations in the L2 in roots and wood than in other organs (Table 3) is due to the presence of calcium carbonate and not more Ca linked to pectins compared to the other studied organs. In this sense, in environments dominated by *Milicia excelsa*, Braissant et al. (2004) reported the presence of calcium carbonate both in the litter and in wood organs as a result of the transformation of calcium oxalate into calcium carbonate

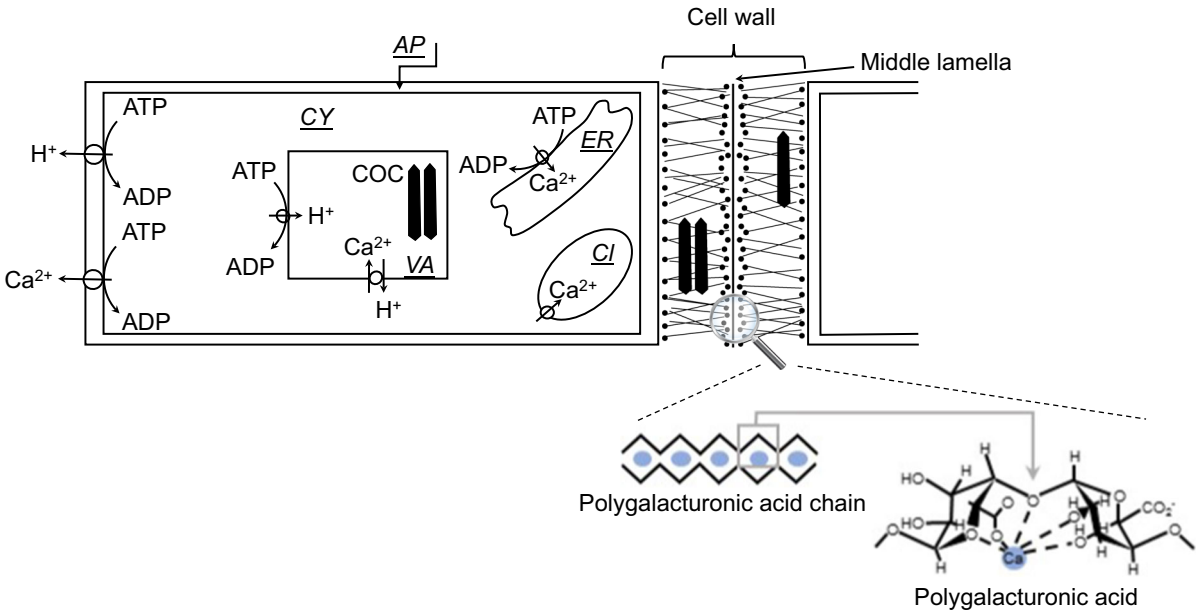

Fig. 6 Schematic illustration of two adjacent cells and localization of Ca^{2+} (adapted from Marschner 1995; White and Broadley 2003; Taiz and Zeiger 2010). High concentrations of Ca are observed in the middle lamella of the cell wall outside the cell, in the endoplasmic reticulum and in the vacuole. Most water-soluble calcium in plant tissues is localized in the vacuole, structurally bound Ca is mainly fixed to polygalacturonic pectin chains in the middle lamella, and insoluble Ca is precipitated in Ca-oxalate crystals. *CY* cytoplasm, *ER* endoplasmic reticulum, *Cl* chloroplast, *VA* vacuole, *COC* Ca-oxalate crystals, *AP* apoplast

through oxalotrophic bacteria. This process was also reported by Verrecchia et al. (1993) to be the cause of some calcrete formation. However, since the root and wood organs also have lower production of COCs compared to other samples, we suggest that they present a greater structurally bound calcium content and that the Ca carbonate crystals represent a minority.

During the third extraction step (L3) using 2 N HCl, which presents the lowest $\delta^{44/40}$Ca isotopic signatures, insoluble Ca originating in Ca-oxalate is extracted (Fink 1991; Borer et al. 2004; Littke and Zabowski 2007; Dauer and Perakis 2014) (Figs. 5, 6). The most important fraction linked to the insoluble Ca is found in bark and leaves (Table 3), which are the organs with a greater production of COCs (Fig. 3b). Ca-oxalate crystals have been observed in several tree organs and species as a mechanism allowing for the sequestration of excess Ca in the cell, with very low Ca concentrations to be maintained in the cytosol, and/or as a fine retardant or defence against herbivores (Franceschi 1989; Kinzel 1989; Desphande and Vishwakarma 1992; Trockenbrodt 1994; Follet-Gueye et al. 1998; Webb 1999; Franceschi 2001; Volk et al. 2002; Hudgins et al. 2003; Dauer and Perakis 2014). When the content of Ca in the apoplast exceeds a certain threshold, exchange sites saturate the wall, the amount of passive Ca streaming to the walls increases, the ability of the cell to compartmentalize the Ca and/or pump it to the apoplast decreases, the levels of free cytosolic Ca increases, and the signal induced by calmodulin initiates the development of the formation of COCs. These changes allow the extraction of Ca from tissues and its chelation in the form of a physiologically and osmotically inactive and insoluble salt. Note that COC formation induces a considerable fractionation amplitude between the water-soluble Ca that can be considered the "Ca source" and the insoluble Ca. Although the fractionation intensity is not constant (between 0.3 and 1.2‰), the following equation always produces ^{40}Ca-enriched crystals:

$$H_2C_2O_4 + Ca^{2+} + nH_2O \rightarrow CaC_2O_4, nH_2O + 2H^+ \quad (4)$$

This study also confirms the earlier hypothesis of the variability of the Ca source at the root level, a variability that is not observable for shoots. Indeed, for wooden roots, the ^{87}Sr/^{86}Sr signature associated with the water-soluble fraction is less radiogenic than the

structurally bound Ca or the Ca precipitated in COCs. This result implies that the source of Sr, and thus Ca circulating in large roots, is different from the immobile Ca from the same organs. In contrast, for small roots, it is the insoluble pool that contains Sr that is more radiogenic. This finding confirms a scatter of Sr, and thus Ca nutrient supply, at least within the same organ, between the apatite-like ($^{87}Sr/^{86}Sr \sim 0.71612$; Aubert et al. 2001) and plagioclase-like ($^{87}Sr/^{86}Sr \sim 0.742$; Probst et al. 2000) soil fractions, as previously suggested (Schmitt et al. 2017).

Characterization of COCs

Infrared spectra and microscopic observations confirmed the presence of COCs and allowed their localization and the identification of their hydration state. In the vegetative and reproductive organs analysed, two COC morphologies were observed: prisms and druses with prominent cores, in coincidence with the research of Lersten and Horner (2008) and Krieger et al. (2017).

Calcium oxalate crystals may occur as mono- or dihydrated. This hydration state depends, among several factors, on the crystalline system in which the crystal forms. Prisms crystallize in the monoclinic system, characteristic of monohydrated crystals (Verrecchia et al. 1993). This crystallization was corroborated from the infrared spectra that showed the presence of monohydrated forms (whewellite) (1315 and 1620 cm^{-1}) mainly in bark and leaves (Maurice-Estepa et al. 2000; Krieger et al. 2017). With regard to druses, they are complex morphologies composed of an aggregate of crystals in any of the hydration states (Verrecchia et al. 1993; Monje and Baran 2002). Although weddellite crystals are less widely distributed in plants, there are reports of their presence (Monje and Baran 2002; Baran and Rolleri 2010; Serdar and Demiray 2012). Nevertheless, we could suggest that druses observed in *Fagus sylvatica* L. could instead represent the most stable form of calcium oxalates (whewellite), as it was corroborated by the infrared spectra analysis (this study) and the XRD analysis in Krieger et al. (2017).

In general, in all organs analysed, crystals are associated with parenchyma, except prisms that are also associated with sclerenchyma tissue. According to Borchert (1984), prisms are associated with suberized and lignified tissues; conversely, druses are associated with cells with thin walls, such as the mesophilic parenchyma cells of leaves. This could be the explanation for the presence of prisms, which are generally associated with vascular and sclerenchyma tissues; and druses with the parenchymatic tissue of both the vegetative and reproductive organs.

In agreement with Lersten and Horner (2008) and Krieger et al. (2017), in leaves of *Fagus* sp., prisms occur along vascular bundles of orders 1 to 3–4, while druses occur in the mesophyll. The differences observed in the density of leaf prismatic crystals could be related to the differential exposure to solar radiation, and thus, to differential transpiration rates. As described above, calcium is absorbed by the roots and distributed to the entire plant through the xylem. The leaves are organs with a high exposure to radiation, so their rate of transpiration is higher than that of other organs. At a higher transpiration rate, calcium accumulates and precipitates as COCs (Franceschi and Nakata 2005; Lersten and Horner 2008; Gilliham et al. 2011), which could explain the higher crystal density in the top leaves and bottom leaves far from the trunk (leaves with higher incidence of solar radiation). Although there are few studies on crystal density, the same pattern in crystal density, size and tissue location in leaves of other arboreal species has been reported. *Eucalyptus globulus*, *Acacia melanoxylon* and *Celtis tala* produce prisms of approximately 10–12 μm and druses of 7.5–15 μm in a range of 120–290 crystals/mm^2 and are mainly associated with vascular bundles and leaf mesophyll (Borrelli et al. 2009).

Geochemical implications

The microscopic results corroborate that the formation of COCs is genetically controlled, so that not only organs but also tissues imply the conditions for the formation of crystals. These patterns agree with the results of the leachate experiments because the organs with a greater proportion of insoluble Ca coincide with the organs with a greater production of COCs. Additionally, the biomineralization process has importance in the isotopic signature of the ecosystem, because it is the fraction where light isotopes prevail. Furthermore, it appears from the combination of Ca isotope measurements, FTIR and microscopic COC characterization that the diversity of the oxalate type is unrelated to isotopic fractionation, suggesting that at

least first order COCs can be considered isotopically, as a whole.

Our leachate experiments show that specific Ca isotopic signatures can be found depending on the considered organ, as well as the Ca speciation within the plant (Fig. 5). Free Ca^{2+} always has greater $\delta^{44/40}$Ca values than structurally bound Ca, and COCs have the lowest $\delta^{44/40}$Ca values within given plant tissues (Fig. 5). This suggests that mineral precipitation induces a higher fractionation intensity between the Ca source and product than the cation-exchange reactions (between 0 and 0.5‰), at least in plants. COC formation is not a randomly occurring process and thus requires the proteins to imitate crystal nucleation and promote crystallization (Addadi and Weiner 1985; Lanzalaco et al. 1988; Bouropoulos et al. 2001; Li et al. 2003). Previous studies considering other isotopic systems (Zn, Cu, Fe, Ni, Si) have noted that the intensity of isotopic fractionation can be explained by coordination number, stoichiometry, cation-O distances, cationic content, and competition between the metal cation and non-acidic neighbouring ligands (Polyakov and Mineev 2000; Dudev and Lim 2004; Shauble 2011; Meheut and Shauble 2014).

Concerning Ca, Colla et al. (2013), experimentally and through calculation, observed variation in the isotopic fractionation intensity between inorganic solids and equilibrating solutions depending on the coordination number of calcium. More recently, Moynier and Fuji (2017), based on ab initio calculations, proposed that a considerable fractionation (up to 3000 ppm) should be observed between various aqueous species of Ca. Thus, $\delta^{44/40}$Ca of COCs precipitated in tree tissues should be 1.6–2.2‰ (depending on hydration coordination and COC species at 25 °C) higher than that of "free" Ca in the transpiration stream. Based on this conclusion, they explained the higher $\delta^{44/40}$Ca values from roots to shoots by COC precipitations in the upper parts of the plants. However, our results as well as the results of a preliminary study (Bullen pers.com.) do not confirm such an interpretation. The $\delta^{44/40}$Ca of COCs are lower than those of free Ca or the Ca linked to pectins. Thus, as we have shown that leaves are enriched in COCs compared to other organs (Table 3, Fig. 2b), if the main cause of the delta Ca variations from roots to shoots were COC precipitation, as suggested by Moynier et al. (2017), the shoots should have lower $\delta^{44/40}$Ca values than the roots, which is not the case.

We therefore propose, as already suggested in Schmitt et al. (2017), another scenario to explain the observed, higher $\delta^{44/40}$Ca values from roots to shoots. Ca circulating in the xylem sap will undergo ionic exchange processes, with ^{40}Ca being preferentially bound to pectins in the middle lamella of the wooden cell wall. Moreover, the suction for the xylem sap circulation in the stem wood is higher than that for the xylem sap circulation in the branch. A slower sap circulation could thus be caused by a higher number of binding sites that could lead to higher $\delta^{44/40}$Ca values at the end of the path, i.e., the leaves.

The results of this study show that Ca isotopic ratios in plants depends on the organ type, as well as the Ca speciation within plants and certainly have implications for the isotopic signature of the recycled Ca in soils from litter decay. Litter decomposition is more rapid for organs with the highest dry matter and nitrogen content and low lignin levels (Berg and Ekbohm 1991; Harmon et al. 1999). Thus, leaves and small roots disappear faster than branches or twigs (John 1973; Rochow 1974).

Different Ca fluxes from different origins can thus be anticipated during litter decomposition. Fraysse et al. (2010) have, for instance, proposed from an experimental study of litter decomposition in temperate and boreal forests that Ca is released in the early stages of dissolution, from the labile reservoirs near the leaf surface, such as Ca linked to pectates (Lodish et al. 1995; Manucharova 2009). When the experiment is continued, intracellular Ca is extracted, possibly including the Ca from oxalate crystals.

In addition, during litter decay, the organic macromolecules are progressively transformed into smaller organic molecules with the formation of recalcitrant chemical components, which can contain Ca. The release of Ca contained in pectin or other organic molecules can thus be delayed during litter decomposition by such a process (Melillo et al. 1989; Berg 2000; Kaiser et al. 2002; Kalbitz and Geyer 2002; Prescott 2010). COCs are fairly insoluble crystals ($K_{sp} = 2.57 \times 10^{-9}$; Ringbom 1963) and can have residence times of several years in soils (Dauer and Perakis (2014). However, there is evidence of the release of COCs from decomposing litter, most often linked to microbial or fungal degradation and/or production (Knutson et al. 1980; Morris and Allen

1994; Canti 2003; Braissant et al. 2004; Verrecchia et al. 2006; Tuason and Arocena 2009; Guggiari et al. 2011; Dauer and Perakis 2014). In addition, the release of oxalic acids into soils by plants and fungi can impact the free soil Ca ions released by litter decay, with the formation of secondary COCs (Oyarbide et al. 2001; Tait et al. 1999; Verrecchia et al. 1993; Jellison et al. 1997; Ryan et al. 2001; Arvieu et al. 2003).

Conclusion

Calcium is distributed in the plant through the transpiration stream. After it enters the cytoplasm, more than 90% of Ca is adsorbed through the cell walls, consistent with the fact that all the studied organs showed the lowest Ca proportion associated with the soluble fraction during our beech tree leachate experiments. In the beech tree organs, Ca can be found mainly enriched in structurally bound Ca or in COCs. Roots and wood are enriched with structurally bound Ca, which provides membrane stability. Bark and leaves are enriched with COCs, which allow excess Ca to be sequestered in the cell, maintaining very low Ca concentrations in the cytosol and defence against herbivores and chewing insects. Finally, reproductive organs are equally enriched in structurally bound Ca and in COCs to ensure the reproductive success of the species (membrane stability and protection against predators). Infrared spectroscopy and COC macropattern descriptions confirm the results of the leachate experiment, with bark and leaves being enriched in COCs compared to other organs. COC observation allowed us to identify prisms and druses in leaves and bark. In leaves, more prisms than druses are observed, suggesting that COCs are mainly whewellite crystals, observable in parenchyma and sclerenchyma tissues. Moreover, leaves with a higher incidence of solar radiation showed larger crystals and a higher crystal density. Our leachate experiments also show that soluble Ca had the greatest $\delta^{44/40}$Ca values, whereas COCs had the lowest. This result could be explained by the difference in equilibrium constants between the isotopologues, a function of the vibrational frequency of the bond. For their part, radiogenic Sr isotopes show a scatter in Sr and Ca nutrient supply within at least one given organ, pointing to source variation. Finally, these experimental observations imply that the $\delta^{44/40}$Ca isotopic signature of litter decomposition depends on the considered organ and the Ca speciation within it. Therefore, to perform the optimal modelling of litter degradation based on seasonal flows, it is now necessary to undergo detailed studies of the different Ca reservoirs and therefore the Ca isotopic variability in the natural environment.

Acknowledgements Colin Fourtet and Eric Pelt are acknowledged for their technical assistance in the laboratory. The manuscript benefitted from constructive reviews by Thomas D. Bullen and an anonymous reviewer. We also thank the editor Jonathan Sanderman for his handling of the manuscript. This project was financially supported by funding from the French CNRS-INSU programme "EC2CO-Cytrix", by the ANPCyT - Argentine (PICT 1583) and the Mar del Plata University - Argentine (EXA 741/2015). This work is an EOST-LHyGeS contribution.

Glossary

Apoplast	Extracellular continuum formed by the pectocellulosic walls and the void spaces between the plant cells. Water and solutes can navigate through non-selective passive diffusion
Chlorenchyma	A chloroplast-containing parenchyma tissue, such as mesophyll and other green tissues (Fahn 1990)
Chloroplast	organelle in which photosynthesis occurs; contains chlorophylls among other pigments (Fahn 1990)
Cortex	The tissue between the vascular cylinder and epidermis of the axis (Fahn 1990)
Cytoplasm	Material within a living cell, excluding the cell nucleus and is approximately 80% water
Endoplasmic reticulum	Type of organelle in eukaryotic cells that, among others, synthesizes proteins
Epidermis	The outermost cell layer of primary tissues of the plant, sometimes comprising more than one layer (Fahn 1990)
Idioblast	Specific cell which is clearly distinguished from the other cells of the tissue in which it appears, either by size, structure or content (Fahn 1990)

Mesophyll	The photosynthetic parenchymatous tissue situated between the two epidermal layers of the leaf (Fahn 1990)
Parenchyma tissue	Ground tissue composed of living cells which may differ in size, shape and wall structure (Fahn 1990)
Phloem	The principal tissue responsible for the transport of assimilates in the vascular plants (Fahn 1990)
Sclerenchyma tissue	A supporting tissue composed of fibres and or sclereids
Vacuole	Eukaryotic cell organelle. In plant cells, this constitutes 80–90% of the volume and weight. It contains mostly water but also organic molecules
Vascular bundle	A strand of conducting tissue in plants (Fahn 1990)
Xylem	The tissue mainly responsible for conduction of water in vascular plants (Fahn 1990)

References

Åberg G, Jacks G, Hamilton PJ (1989) Weathering rates and $^{87}Sr/^{86}Sr$ ratios: an isotopic approach. J Hydrol 109:65–78

Addadi L, Weiner S (1985) Interactions between acidic proteins and crystals: stereochemical requirements in biomineralization. Proc Natl Acad Sci USA 82:4110–4114

Amtmann A, Blatt MR (2009) Regulation of macronutrient transport. New Phytol 181:35–52

Arvieu JC, Leprince F, Plassard C (2003) Release of oxalate and protons by ectomycorrhizal fungi in response to P-deficiency and calcium carbonate in nutrient solution. Ann For Sci 60:815–821

Aubert D, Stille D, Probst A (2001) REE fractionation during granite weathering and removal by waters and suspended load: Sr and Nd isotopic evidence. Geochim Cosmochim Acta 65:387–406

Bagard ML, Schmitt AD, Chabaux F et al (2013) Biogeochemistry of stable Ca and radiogenic Sr isotopes in a larch-covered permafrost-dominated watershed of Central Siberia. Geochim Cosmochim Acta 114:169–187

Bailey SW, Hornbeck JW, Driscoll CT et al (1996) Calcium inputs and transport in a base-poor forest ecosystem as interpreted by Sr isotopes. Water Resour Res 32:707–719

Bailey SM, Buso DC, Likens GE (2003) Implications of sodium mass balance for interpreting the calcium cycle of a forested ecosystem. Ecology 84:471–484

Bangerth F (1979) Calcium related physiological disorders of plants. Ann Rev Phytopathol 17:97–122

Baran EJ, Rolleri CH (2009) IR-spectroscopic characterization of biominerals in the marattiaceaeus ferns. Rev Bras Bot 33:519–523

Baran EJ, Rolleri CH (2010) IR-spectroscopic characterization of biominerals in marattiaceaus ferns. Rev Bras Bot 33:519–523

Baran EJ, Gonzales-Baro AC, Ciciarelli MM et al (2010) Characterization of biominerals in species of Canna (Cannaceae). Rev Biol Trop (Int J Trop Biol) 58:1507–1515

Bauer P, Elbaumb R, Weissc I (2011) Calcium and silicon mineralization in land plants: transport, structure and function. Plant Sci 180:746–756

Bedel L, Poszwa A, Van Der Heijden G et al (2016) Unexpected calcium sources in deep soil layers in low-fertility forest soils identified by strontium isotopes (Lorraine plateau, eastern France). Geoderma 264:103–116

Bélanger N, Holmden C, Courchesne F et al (2012) Constraining soil mineral weathering $^{87}Sr/^{86}Sr$ for calcium apportionment studies of a deciduous forest growing on soils developed from granitoid igneous rocks. Geoderma 185:84–96

Belliveau J, Griffin H (2001) The solubility of calcium oxalate in tissue culture media. Anal Biochem 291:69–73

Berg B (2000) Litter decomposition and organic matter turnover in northern forest soils. For Ecol Manag 133:12–22

Berg B, Ekbohm G (1991) Litter mass-loss rates and decomposition patterns in some needle and leaf litter types. Long-term decomposition in a Scots pine forest. Can J Bot 69:1449–1456

Blum JD, Klaue A, Nezat CA et al (2002) Mycorrhizal weathering of apatite as an important calcium source in base-poor forest ecosystems. Nature 417:729–731

Borchert R (1984) Functional anatomy of the calcium excreting system of *Gleditsia triacanthos* L. Bot Gaz 145:474–482

Borer CH, Schaberg PG, DeHaynes DH et al (2004) Accretion, partitioning and sequestration of calcium and aluminium in red spruce foliage: implications for tree health. Tree Phys 24:929–939

Borrelli NL, Osterrieth M, Oyarbide F et al (2009) Calcium biominerals in typical Argiudolls from the Pampean Plain, Argentina: an approach to the understanding of their role within the calcium biogeochemical cycle. Quat Int 193:61–69

Bouropoulos N, Weiner S, Addadi L (2001) Calcium oxalate crystals in tomato and tobacco plants: morphology and in vitro interactions of cristal associated macromolecules. Chemistry 7:1881–1888

Boutin R, Montigny R, Thuizat R (1995) Chronologie K-Ar et $^{39}Ar/^{40}Ar$ du métamorphisme et du magmatisme des Vosges. Comparaison avec les massifs varisques avoisinants. Géol Fr 1:3–25

Bozarth SR (1990) Diagnostic opal phytoliths from pods of selected varieties of common beans (*Phaseolus vulgaris*). Am Antiq 55:98–104

Braissant O, Cailleau G, Aragno M et al (2004) Biologically induced mineralization in the iroko *Milicia excelsa* (*Moraceae*): its causes and consequences to the environment. Geobiology 2:59–66

Bullen TD, Bailey SW (2005) Identifying calcium sources at an acid deposition-impacted spruce forest: a strontium isotope, alkaline earth element multi-tracer approach. Biogeochem 74:63–99

Caldwell CR, Haug A (1981) Temperature dependence of the barley root membrane bound Ca^{2+} and Mg^{2+}-depedent ATPase. Physiol Plant 53:117–124

Canti MG (2003) Aspects of the chemical and microscopic characteristics of plant ashes found in archaeological soils. Catena 54:339–361

Capo RC, Stewart BW, Chadwick OA (1998) Strontium isotopes as tracers of ecosystem process: theory and methods. Geoderma 82:190–225

Catinon M, Ayrault S, Daudin L et al (2008) Atmospheric inorganic contaminants and their distribution inside stem tissues of *Fraxinus excelsior* L. Atmos Environ 42:1223–1238

Christy AC, Nodland E, Burnham AK et al (1994) Determination of kinetic parameters for the dehydration of calcium oxalate monohydrate by diffuse reflectance FT-IR spectroscopy. Appl Spectrosc 48:561–568

Clarkson DT (1984) Calcium transport between tissues and its distribution in the plant. Plant Cell Environ 7:449–456

Cobert F, Schmitt AD, Bourgeade P et al (2011) Experimental identification of Ca isotopic fractionations in higher plants. Geochim Cosmochim Acta 75:5467–5482

Colla ChA, Wimpenny J, Yin QZ et al (2013) Calcium-isotope fractionation between solution and solids with six, seven, or eight oxygen bounds to Ca(II). Geochim Cosmochim Acta 121:363–373

Contreras-Padilla M, Rivera-Munos EM, Gutierrez-Cortez E et al (2015) Characterization of crystalline structures in *Opuntia ficus-indica*. J Biol Phys 41:99–112

Cromack K Jr, Sollins P, Graustein W et al (1979) Calcium oxalate accumulation and soil weathering in mats of the hypogenous fungus *Hysterangium crissum*. Soil Biol Biochem 11:463–468

Dauer JM, Perakis SS (2013) Contribution of calcium oxalate to soil-exchangeable calcium. Soil Sci 178:671–678

Dauer JM, Perakis SS (2014) Calcium oxalate contribution to calcium cycling in forests of contrasting nutrient status. For Ecol Manag 334:64–73

Desphande BP, Vishwakarma AK (1992) Calcium oxalate crystals in the fusiform cells of the cambium of *Gemelina arborea*. IAWA Bull 13:297–300

Dijkstra FA (2003) Calcium mineralization in the forest floor and surface soil beneath different tree species in the northeastern US. For Ecol Manag 175:185–194

Dizeo de Strittmater CG (1973) Nueva técnica de diafanización. Bol Soc Argent Bot 15:126–129

Drouet T, Herbauts J, Gruber W et al (2005) Strontium isotope composition as a tracer of calcium sources in two forest ecosystems in Belgium. Geoderma 126:203–223

Dudev T, Lim C (2004) Oxyanion selectivity in sulfate and molybdate transport proteins: an ab initio ICDM study. J Am Chem Soc 120:10296–10305

Eisenhauer A, Nägler T, Stille P et al (2004) Proposal for an international agreement on Ca notations resulting from discussions at workshops on stable isotope measurements held in Davos (Goldschmidt 2002) and Nice (EGS–AGU–EUG 2003). Geostand Geoanal Res 28:149–151

Epstein E, Bloom AJ (2005) Mineral nutrition of plants: principles and perspectives, 2nd edn. Sinauer Associates, Sunderland, p 405p

Fahn A (1990) Plant anatomy. Pergamon Press, Oxford

Fichter J, Turpault MP, Dambrine E et al (1998a) Localization of base cations in particle size fractions of acid forest soils, Vosges Mountains, N-E France. Geoderma 82:295–314

Fichter J, Turpault MP, Dambrine E et al (1998b) Mineral evolution of acid forest soils in the Strengbach catchment (Vosges Mountains, N-E France). Geoderma 82:315–340

Fink S (1991) The micromorphological distribution of bound calcium in needles of Norway spruce [*Picea abies* (L.) Karst.]. New Phytol 119:33–40

Follet-Gueye ML, Verdus MC, Demarty M et al (1998) Cambium pre-activation in beech correlates with a strong temporary increase of calcium in cambium and phloem but not in xylem cells. Cell Calc 24:205–211

Franceschi VR (1989) Calcium oxalate formation is a rapid and reversible process in *Lemna minor* L. Protoplasma 148:130–137

Franceschi V (2001) Calcium oxalate in plants. Trends Plant Sci 7:331

Franceschi VR, Nakata PA (2005) Calcium oxalate in plants: formation and function. Ann Rev Plant Biol 56:41–71

Fraysse F, Pokrovsky O, Meunier JD (2010) Experimental study of terrestrial plant litter interaction with aqueous solutions. Geochim Cosmochim Acta 74:70–84

Gadd GM (1999) Fungal production of citric and oxalic acid: importance in metal speciation, physiology and biogeochemical processes. Adv Microb Physiol 41:47–92

Gangloff S, Stille P, Schmitt AD et al (2016) Factors controlling the chemical compositions of colloidal and dissolved fractions in soil solutions and the mobility of trace elements in soils. Geochim Cosmochim Acta 189:37–57

Gilliham M, Dayod M, Hocking BJ et al (2011) Calcium delivery and storage in plant leaves: exploring the link with water flow. J Exp Bot 62:2233–2250

Graustein WC (1989) $^{87}Sr/^{86}Sr$ ratios measure the sources and flow of strontium in terrestrial ecosystems. In: Rundel PW, Ehleringer JR, Nagy KA (eds) Stable isotopes in ecological research. Springer, Berlin, pp 491–512

Grinand C, Barthès BG, Brunet D et al (2012) Prediction of soil organic and inorganic carbon contents at a national scale (France) using mid-infrared reflectance spectroscopy (MIRS). Eur J Soil Sci 63:141–151

Guggiari M, Bloque R, Aragno M et al (2011) Experimental calcium-oxalate crystal production and dissolution by selected wood-rot fungi. Int Biodeterior Biodegrad 65:803–809

Harmon ME, Nadelhoffer KJ, Blair JM (1999) Measuring decomposition, nutrient turnover, and stores in plant litter. In: Robertson GP, Coleman DC (eds) Standard soil methods for long-term ecological research. Oxford University Press, Oxforf, pp 202–240

Hippler D, Schmitt AD, Gussone N et al (2003) Calcium isotopic composition of various reference materials and seawater. Geostand Newsl 27:13–19

Horner HT (2012) *Peperomia* leaf cell wall interface between the multiple hypodermis and crystal-containing photosynthetic layer displays unusual pit fields. Ann Bot 109:1307–1315

Hudgins JW, Krekling T, Franceschi VR (2003) Distribution of calcium oxalate crystals in the secondary phloem of conifers: a constitutive defense mechanism? New Phytol 159:677–690

Ilarslan H, Palmer RG, Imsande J et al (1997) Quantitative determination of calcium oxalate and oxalate in developing seeds of soybean (Leguminosae). Am J Bot 84:1042–1046

Inanaga S, Okasaka A (1995) Calcium and silicon binding compounds in cell walls of rice shoots. Soil Sci Plant Nutr 41:103–110

Ito A, Fujiwara A (1968) The relation between calcium and cell wall in growing rice leaf. Plant Cell Physiol 9:433–439

Jellison J, Connolly J, Goodell B, Doyle B, Illman B, Fekete F, Ostrofsky A (1997) The role of cations in the biodegradation of wood by the brown rot fungi. Int Biodeterior Biodegrad 39:165–179

John DM (1973) Accumulation and decay of litter and net production of forest in tropical west Africa. Oikos 24:430–435

Kaiser K, Guggenberger G, Haumaier L et al (2002) The composition of dissolved organic mater in forest soil solutions: changes induced by seasons and passage through the mineral soil. Org Geochem 33:307–318

Kalbitz K, Geyer G (2002) Different effects of peat degradation on dissolved organic carbon and nitrogen. Org Geochem 33:319–326

Kamatani A (1991) Physical and chemical characteristics of biogenous silica. Mar Biol 8:89–95

Kendall C, Sklash MG, Bullen TD (1995) Isotope tracers of water and solute sources in catchments. Solute modelling in catchment systems. Wiley, New York, pp 261–303

Kennedy MJ, Hedin LO, Derry LA (2002) Decoupling of unpolluted temperate forests from rock nutrient sources revealed by natural $^{87}Sr/^{86}Sr$ and ^{84}Sr tracer addition. Proc Natl Acad Sci 99:9639–9644

Kinzel H (1989) Calcium in the vacuoles and cell walls of plant tissue. Flora 182:99–125

Knutson DM, Hutchins AS, Cromack K (1980) The association of calcium oxalate-utilizing Streptomyces with conifer ectomycorrhizae. Antoine van Leenwenhoek 46:611–619

Korth K, Doege SJ, Park SH et al (2006) *Medicago truncatula* mutants demonstrate the role of plant calcium oxalate crystals as an effective defense against chewing insects. Plant Phys 141:188–195

Krieger C, Calvaruso C, Morlot C et al (2017) Identification, distribution and quantification of biominerals in a deciduous forest. Geobiology 15:296–310

Lahd Geagea M, Stille P, Millet M et al (2007) REE characteristics and Pb, Sr and Nd isotopic compositions of steel plant emissions. Sci Tot Environ 373:404–419

Lahd Geagea M, Stille P, Gauthier-Lafaye F et al (2008) Baseline determination of the atmospheric Pb, Sr and Nd isotopic compositions in the Rhine Valley, Vosges Mountains (France) and the Central Swiss Alps. Appl Geochem 23:1704–1714

Lanzalaco AC, Singh PB, Smesko SA et al (1988) The influence of urinary macromolecules of calcium oxalate monohydrate crystal growth. J Urol 193:190–195

Lersten NR, Horner HT (2008) Crystal macropatterns in leaves of Fagaceae and Nothofagaceae: a comparative study. Plant Syst Evol 271:239–253

Li X, Zhang D, Lynch-Holm VM et al (2003) Isolation of a crystal matrix protein associated with calcium oxalate precipitation in vacuoles of specialized cells. Plant Physiol 133:549–559

Liao JD, Boutton TW, Jastrow JD (2006) Organic matter turnover in soil physical fractions following woody plant invasion of grassland: evidence from natural ^{13}C and ^{15}N. Soil Biol Biochem 38:3197–3210

Likens GE, Driscoll CT, Buso DC et al (1998) The biogeochemistry of calcium at Hubbard Brook. Biogeochemistry 41:89–173

Littke KM, Zabowski D (2007) Influence of calcium fertilization on Douglas-fir foliar nutrition, soil nutrient availability and sinuosity in coastal Washington. For Ecol Manag 247:140–148

Lodish H, Baltimore D, Berk A et al (1995) Molecular cell biology, 3rd edn. New York, Freeman

Manucharova NA (2009) The microbial destruction of chitin, pectin, and cellulose in soils. Soil Boil 42:1526–1532

Marschner H (1995) Mineral nutrition of higher plants, 2nd edn. Academic Press, London

Maurice-Estepa L, Levillain P, Lacour B et al (2000) Advantage of zero-crossing-point first-derivative spectrophotometry for the quantification of calcium oxalate crystalline phases by infrared spectrophotometry. Clin Chim Acta 298:1–11

McLaughlin SB, Wimmer R (1999) Tansley review no 104 Calcium physiology and terrestrial ecosystem processes. New Phytol 142:373–417

Meheut M, Shauble EA (2014) Silicon isotope fractionation in silicate minerals: insights from first-principles models of phyllosilicates, albite and pyrope. Geochim Cosmochim Acta 134:137–154

Melillo JM, Aber JD, Linkins AE et al (1989) Carbon and nitrogen dynamics along the decay continuum: plant litter to soil organic matter. Plant Soil 115:189–198

Mendham J, Denney R, Barnes J et al (2000) Vogel's quantitative chemical analysis, 6th edn. Prentice Hall, New York

Miller EK, Blum JD, Friedland AJ (1993) Determination of soil exchangeable-cation loss and weathering rates using Sr isotopes. Nature 362:438–441

Molano-Flores B (2001) Herbivory and calcium concentrations affect calcium oxalate crystal formation in leaves of *Sida* (Malvaceae). Ann Bot 88:387–391

Monje PV, Baran EJ (1996) On the formation of weddellite in *Chamaecereus silvestrii*, a Cactaceae species from northern Argentina. Z Naturforsch 51c: 426-428

Monje PV, Baran EJ (1997) On the formation of whewellite in the Cactaceae species *Opuntia microdasys*. Z Naturforsch 52c:267–269

Monje P, Baran E (2002) Characterization of calcium oxalates generated as biominerals in cacti. Plant Physiol 128:707–713

Monje PV, Baran EJ (2004) Complex biomineralization pattern in cactaceae. J Plant Phys 161:121–123

Monje PV, Baran EJ (2005) Evidence of the formation of glushinkite as a biomineral in a Cactaceae species. Phytochemistry 66:611–614

Morris SJ, Allen MF (1994) Oxalate-metabolizing microorganisms in sagebrush steppe soil. Biol Fertil Soils 18:255–259

Moynier F, Fuji T (2017) Calcium isotope fractionation between aqueous compounds relevant to low-temperature geochemistry, biology and medicine. Sci Rep Nat. https://doi.org/10.1038/srep44255

Oyarbide F, Osterrieth M, Cabello M (2001) *Trichoderma koningii* as a biomineraliziting fungous agent of calcium oxalate crystals in typical Argiudolls of the Los Padres Lake natural reserve (Buenos Aires, Argentina). Microbiol Res 156:1–7

Perry CC (1989) Chemical studies of biogenic silica. In: Mann S, Webb J, Williams RJP (eds) Biomineralization: chemical and biochemical perspectives. Verlag, Weinheim, pp 223–256

Pilbeam DJ, Morley PS (2007) Calcium. In: Barker AV, Pilbeam DJ (eds) Handbook of plant nutrition. CRC Press, Boca Raton, pp 121–144

Polyakov VB, Mineev SD (2000) The use of Mössbauer spectroscopy in stable isotope geochemistry. Geochim Cosmochim Acta 64:849–865

Prescott C (2010) Litter decomposition: what controls it and how can we alter it to sequester more carbon in forest soils? Biogeochemistry 101:133–149

Probst A, Dambrine E, Viville D et al (1990) Influence of acid atmospheric inputs on surface water chemistry and mineral fluxes in a declining spruce stand within a small granitic catchment (Vosges massif-France). J Hydrol 116:101–124

Probst A, El Gh'Mari A, Aubert D et al (2000) Strontium as tracer of weathering processes in a silicate catchment polluted by acid atmospheric inputs, Strengbach, France. Chem Geol 170:203–219

Prunier J, Chabaux F, Stille P et al (2015) Chemical and isotopic (Sr, U) monitoring of soil solutions from the Strengbach catchment (Vosges mountains, France), evidence for recent weathering evolution. Chem Geol 417:289–305

Prychid CJ, Rudall PJ (1999) Calcium oxalate crystals in monocotyledons: a review of their structure and systematics. Ann Bot 84:725–739

Ringbom A (1963) Complexation in analytical chemistry. Interscience, New-York

Roberts DM, Besl L, Oh SH et al (1992) Expression of a calmodulin methylation mutant affects the growth and development of transgenic tobacco plants. Proc Natl Acad Sci USA 89:8394–8398

Rochow JJ (1974) Litter fall relations in a Missouri Forest. Oikos 25:80–85

Ryan PR, Delhaize E, Jones DL (2001) Function and mechanisms of organic anion exudation from plant roots. Ann Rev Plant Phys Plant Mol Biol 52:527–560

Schmitt AD, Gangloff S, Cobert F et al (2009) High performance automated ion chromatography separation for Ca isotope measurements in multiple natural matrices. J Anal At Spectrom 24:1089–1097

Schmitt AD, Vigier N, Lemarchand D et al (2012) Processes controlling the stable isotope compositions of Li, B, Mg and Ca in plants, soils and waters: a review. C R Géosci 344:704–722

Schmitt AD, Cobert F, Bourgeade P et al (2013) Calcium isotope fractionation during plant growth under a limiting nutrient supply. Geochim Cosmochim Acta 110:70–83

Schmitt AD, Gangloff S, Labolle F et al (2017) Calcium biogeochemical cycle at the beech tree-soil solution interface from the Strengbach CZO (NE France): insights from stable Ca and radiogenic Sr isotopes. Geochim Cosmochim Acta 213:91–109

Serdar B, Demiray H (2012) Calcium oxalate crystal types in three oak species (*Quercus* L.) in Turkey. Turk J Biol 36:386–393

Shauble EA (2011) First-principles estimates of equilibrium magnesium isotope fractionation in silicate, oxide, carbonate and hexaaquamagnesium (2+) crystals. Geochim Cosmochim Acta 75:844–869

Tait K, Sayer J, Gharieb M et al (1999) Fungal production of calcium oxalate in leaf litter microcosms. Soil Biol Biochem 31:1189–1192

Taiz L, Zeiger E (2010) Plant physiology, 5th edn. Sinauer Associates Inc., Sunderland

Trockenbrodt M (1994) Quantitative changes of some anatomical characters during bark development in *Quercus robur*, *Ulmus glabra*, *Populus tremula* and *Betula pendula*. IAWA J 15:387–398

Trockenbrodt M (1995) Calcium oxalate crystals in the bark of *Quercus robur*, *Ulmus glabra*, *Populus tremula* and *Betula pendula*. Ann Bot 75:281–284

Tuason MMS, Arocena JM (2009) Calcium oxalate biomineralization by *Piloderma fallax* in response to various levels of calcium and phosphorus. Appl Environ Mircobiol 75:7079–7085

Verrecchia EP, Dumont JL, Verrecchia KE (1993) Role of calcium oxalate biomineralization by fungi in the formation of calcretes: a case study from Nazareth. Isr J Sediment Pet 63:1000–1006

Verrecchia EP, Braissant O, Cailleau G (2006) The oxalate-carbonate pathway in soil carbon storage: the role of fungi and oxalotrophic bacteria. In: Gadd M (ed) Fungi in biogeochemical cycles. Cambridge University Press, Cambridge, pp 289–310

Viville D, Chabaux F, Stille P et al (2012) Erosion and weathering fluxes in granitic basins: example of the Strengbach catchment (Vosges massif, Eastern France). CATENA 92:122–129

Volk GM, Lynch-Holm VJ, Kostman TA et al (2002) The role of druse and raphide calcium oxalate crystals in tissue calcium regulation in *Pistia stratiotes* leaves. Plant Biol 4:34–45

Webb MA (1999) Cell-mediated crystallization of calcium oxalate in plants. Plant Cell 11:751–761

White PJ, Broadley MR (2003) Calcium in plants. Ann Bot 92:487–511

Willats WG, McCartney L, Mackie W et al (2001) Pectin: cell biology and prospects for functional analysis. Plant Mol Biol 47:9–27

WRB (2014) World reference base for soil resources 2014. International soil classification system for naming soils and creating legends for soil maps. Update 2015. www.fao.org/3/a-i3794e.pdf

Zar JH (1984) Biostatistical analysis. Prentice-Hall, Englewood Cliffs